

The Pacific QDO as a Natural Predictor for the Great Salt Lake Elevation

Robert R. Gillies and Shih-Yu Wang

Utah Climate Center/Department of Plants, Soils, and Climate

Utah State University, Logan, UT

1. Introduction

The lake elevation of the Great Salt Lake (GSL), a large closed basin in the arid western United States, is characterized by a pronounced quasi-decadal oscillation (QDO) (Lall and Mann 1995). Wang *et al.* (2009a) found that the variation of the GSL elevation is very coherent with the QDO of sea surface temperature anomalies in the tropical central Pacific, known as the Pacific QDO (White and Liu 2008a, b). The Pacific QDO can be depicted by the SST anomalies in the NINO4 region (Allan 2000), denoted as Δ SST (NINO4). Fig. 1 illustrates the coherence between the GSL elevation and Δ SST (NINO4). However, such a coherence denies any direct association between the precipitation over the GSL watershed and the Pacific QDO because, in a given frequency, the precipitation variations always lead the GSL elevation variations. In other words, a direct link between the Pacific QDO and the precipitation source of the GSL is absent. What causes the GSL elevation to vary so coherently with Δ SST (NINO4) is therefore an intriguing question.

A pronounced quasi-decadal variability was observed in the Intermountain precipitation (*cf.* Fig.2c) as well as the GSL elevation (*cf.* Fig. 2b). Wang *et al.* (2009a) noted that the precipitation QDO in the Intermountain region consistently lags the Pacific QDO by a quarter-phase, *i.e.* 3 years after the peak of the warm-phase Pacific QDO occurs, an anomalous trough develops over the Gulf of Alaska and enhances the Intermountain precipitation. For the opposite, the cool-phase Pacific QDO, 3 years later an anomalous ridge forms in the same location and thus reduces the Intermountain precipitation. These findings lead to a hypothesis that the quasi-decadal coherence between Δ SST (NINO4) and the GSL elevation, as described in Fig. 1, reflects a sequential process that begins with the warm/cool phase of the Pacific QDO and ultimately affects the GSL elevation, through modulations of the quadrature amplitude modulation of the Pacific QDO on the intermountain precipitation. Here we examine this hypothesis by analyzing the meteorological and hydrological variables over the Great Basin.

2. Data

Gridded data used in the analysis included the Kaplan Extended SST (Kaplan *et al.* 1998), the U.K. Meteorological Office Hadley Centre's mean sea level pressure (HadSLP2; Allan and Ansell 2006), the NCEP/NCAR Global Reanalysis (Kalnay *et al.* 1996), and the gauge-based monthly precipitation (Legates and Willmott 1990), all of which were provided through the NOAA/OAR/ESRL PSD. Lake elevations of the GSL over the period of record were obtained from the United States Geological Survey (USGS). This

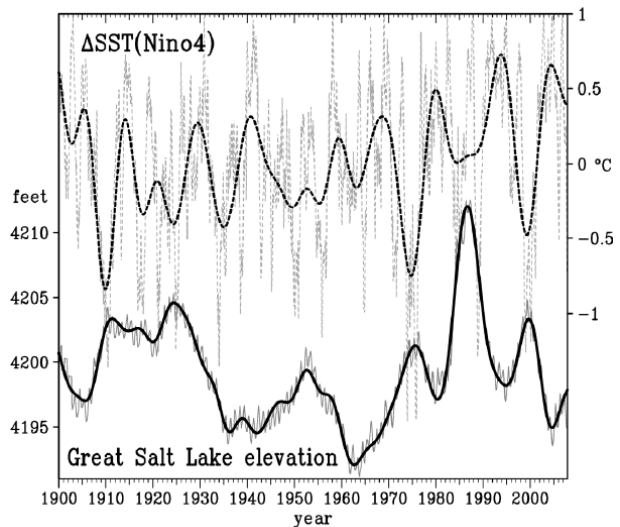


Fig. 1. Monthly GSL elevation (in feet; thick solid curve) and the Kaplan SST anomalies ($^{\circ}$ C) in the NINO4 region (160° E- 150° W, 5° S- 5° N) denoted as Δ SST(NINO4) (thick dashed curve), both were smoothed by a 6 year lowpass. The original time series of the GSL elevation and Δ SST (NINO4) are superimposed as gray thin curve and gray dashed curve, respectively.

study used the post-1900 records of the GSL elevation measured at the Boat Harbor location southwest of the GSL.

3. Results

a. Statistics

Power spectrums of the monthly unfiltered Δ SST (NINO4), the GSL elevation, and the precipitation within the hydrological drainage basin of the GSL are given in Fig. 2a-c. Significant signals between 10 and 15 years are clearly visible. To examine the apparent association between Δ SST (NINO4) and the GSL elevation as noted in Fig. 1, we performed the multitaper method (MTM) of spectral coherence analysis (Mann and Park 1996) on both the GSL elevation and Δ SST (NINO4) over the period of record from 1900 to 2007. As shown in Fig. 2d, a high degree of coherence between the GSL elevation and Δ SST (NINO4) stands out in the 10-15 year frequency domain. The peak of this quasi-decadal coherence is significant at the 95% confidence level with a near 180° phase difference, supporting the out-of-phase relationship as was revealed in Fig. 1. The MTM coherence between Δ SST (NINO4) and the GSL elevation tendency (Fig. 2e) resembles Fig. 2d, except for a 90° phase difference in the 10-15 year frequency domain. These features were also observed in Fig. 2f, as the coherence between Δ SST (NINO4) and the precipitation is significant at the 99% confidence level. The compilation of results in Fig. 2 indicates that the Pacific QDO leads both the precipitation and the GSL elevation tendency by a quarter-phase. Because the GSL elevation tendency follows the precipitation which leads the GSL elevation by another quarter-phase, the GSL elevation should lag Δ SST(NINO4) by a half-phase (180°) in this quasi-decadal time scale.

To substantiate the analysis given in Fig. 2, monthly time series of Δ SST (NINO4), the precipitation, and the GSL elevation were subsequently filtered using the Hamming-Windowed filter (Iacobucci and Noullez 2005) within the 10-15 year frequency band, the result of which is given in Fig. 3. The warm, cool, rising and falling transition phases of the QDO evolution in Δ SST (NINO4) are illustrated along with the precipitation and the GSL elevation. Immediately obvious is that all three time series exhibit clear quasi-

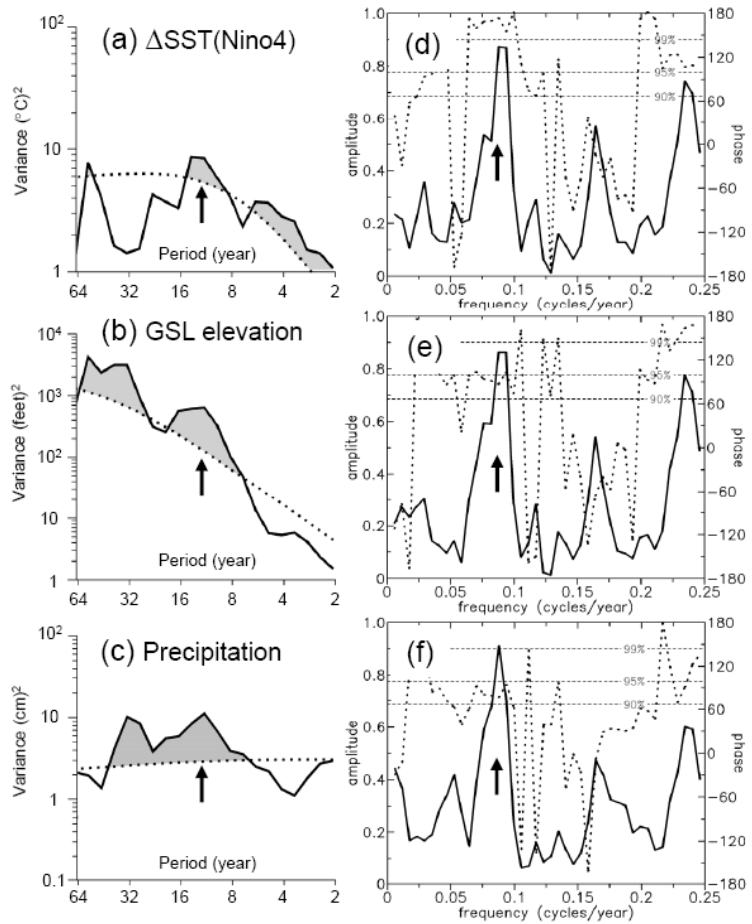


Fig. 2. The global wavelet power spectrum of monthly unfiltered (a) Δ SST (NINO4), (b) GSL elevation, and (c) precipitation within the GSL hydrological drainage basin from 1900 to 2007. (d), (e), (f) MTM coherence (solid curve) and phase (dotted curve) between Δ SST (NINO4) and the GSL elevation (d), the GSL elevation tendency (e), and Precipitation (f) respectively using three 2π tapers. Dotted lines in (a)-(c) indicate the 99% significance level determined by a red-noise (autoregressive lag 1) background spectrum. The dashed horizontal lines in (d)-(f) are the 90%, 95%, and 99% confidence limits for the coherence amplitude. Note that the phase lags of 180° and -180° are the same. The phase difference at $0.075 < f < 0.1$ in (e) and (f) has Δ SST (NINO4) leading the GSL elevation tendency and the precipitation, respectively.

decadal variabilities, despite a somewhat inactive period in 1945-1960. As previously mentioned, the evolution of the three fields is linked from one to another, i.e. 3 years after the peak warm phase of the Pacific QDO [Δ SST (NINO4)], the precipitation reaches its maximum; another 3 years after the precipitation peak, the GSL elevation attains its peak – as illustrated by dashed gray arrows in Fig. 3. The process for the GSL elevation to respond to Δ SST (NINO4) therefore spans a approximate 6 years, equivalent to a half-phase (180°) of the ~ 12 year frequency.

b. Dynamics

In order to examine the possible teleconnection associated with the Pacific QDO as was revealed by the statistical analysis, composites of gridded sea level pressure (SLP) and precipitation were compiled for the cold season (November-March) during the warm and cool phases of the Pacific QDO.

These phases were defined by the bandpassed Δ SST (NINO4) as an index (*cf.* Fig. 3). The warm and cool phases were determined by the years when the Δ SST (NINO4) index is above and below 0.8 standard deviation, respectively, namely the high-index and low-index years. The differences in the composite precipitation and SLP patterns between the high-index and low-index years are shown in Fig. 4a (years given in the caption). The north-south precipitation pattern across the Intermountain region, as well as an anomalous low-pressure cell in the subtropical Eastern Pacific, is typical to those associated with the warm-phase ENSO and the positive-phase PDO (Dettinger *et al.* 1998; Gershunov and Barnett 1998). However, the GSL lies in the transitional zone of this north-south precipitation pattern, where the effect of the extreme phase of the Pacific QDO is weak. Using the high-/low-index years *plus 3 years* (i.e. a quarter-phase lagging the extreme phase), the composite precipitation and SLP patterns (Fig. 4b) shift northward about 15° in latitude, with the maximum amplitudes of precipitation and SLP positioned near their zero contours as in Fig. 4a. The shifting in the circulation and precipitation patterns indicates a sequential evolution from the warm-phase Pacific QDO to the transition-phase Pacific QDO. Specifically during the warm-to-cool transition phase of the Pacific QDO, the low-pressure cell has moved northward to a location near the Gulf of Alaska, leading to positive precipitation anomalies over the GSL watershed (Fig. 4b).

The results such as those presented in Figs. 3 and 4 suggest a large-scale teleconnection pattern associated with the transition phases of the Pacific QDO. The warm and cool phases of the Pacific QDO feature an ENSO-like SST pattern (Zhang *et al.* 1997) and subsequently an ENSO-like circulation pattern. On the other hand, Wang *et al.* (2009b) found that the SST pattern during the transition phases of the Pacific QDO redistributes heating anomalies of the SST and tropical convection which, in turn, induce a teleconnection wave train emanating from the tropical Western Pacific toward the Gulf of Alaska. These SST and atmospheric circulation patterns are shown in Fig. 5 through two independent rotated EOF analyses. Note that the atmospheric circulation here is represented by the streamfunction of column-integrated water vapor flux (ψ_Q ; Chen 1985) in order to better depict the tropical circulation. The strongly correlated coefficients of these two EOFs (Fig. 5e and 5f) indicate that the SST and the teleconnection patterns are coupled. However, the transition-phase circulation pattern (Fig. 5d) is far weaker than the extreme-phase

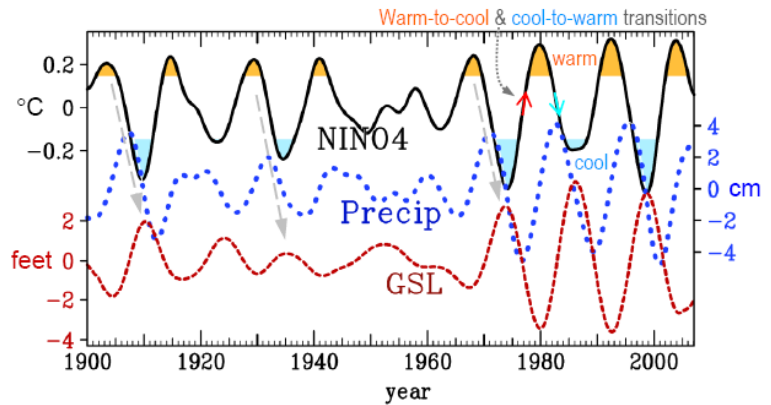


Fig. 3. Time series of bandpassed Δ SST (NINO4) (black solid curve), precipitation over the Great Basin (blue dotted curve), and the GSL elevation (red dashed curve) from 1900 to 2007 using the HW filter with the 10-15 yr frequency. Orange (cyan) shadings in Δ SST (NINO4) indicate years when Δ SST is above (below) the 0.8 standard deviation from the mean. These years are used for the composite analysis in Fig. 4. Gray dashed arrows describe the time lag evolution from Δ SST (NINO4) to the precipitation and then to the GSL elevation. The phases of the Pacific QDO are explained with the Δ SST (NINO4) index.

one (Fig. 5c), corresponding to their associated SST patterns (Figs. 5a and 5b). Nonetheless, the teleconnection wave train during the transition-phase Pacific QDO is persistent and has direct impact on the Intermountain precipitation regime (Wang *et al.* 2009b). This forms the source of quasi-decadal signals recorded for the Intermountain precipitation as well as the GSL elevation.

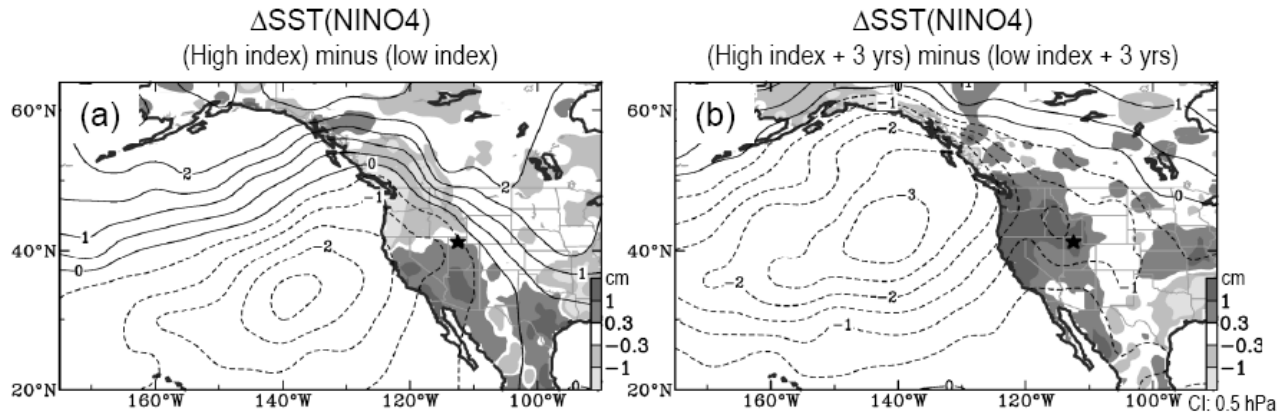


Fig. 4. (a) Differences in precipitation (U. Delaware; shadings) and SLP (HadSLP2; contours) between composites of high-index years (1902-04, 1914-16, 1928-30, 1940-42, 1967-69, 1978-81, 1991-94, and 2003-05) and low-index years (1909-11, 1923, 1934-36, 1973-75, 1985-87, and 1997-2000) during the cold season (November of the previous year to March), based on the bandpassed $\Delta\text{SST}(\text{NINO4})$ in Fig. 3. The contour interval of SLP is 0.5 hPa while precipitation below the 95% confidence level (t -test) is omitted. (b) Same as (a) but for the composites between high- and low-index years plus 3 years. Data are unfiltered. The GSL is indicated by a star. Significance level of SLP is not shown.

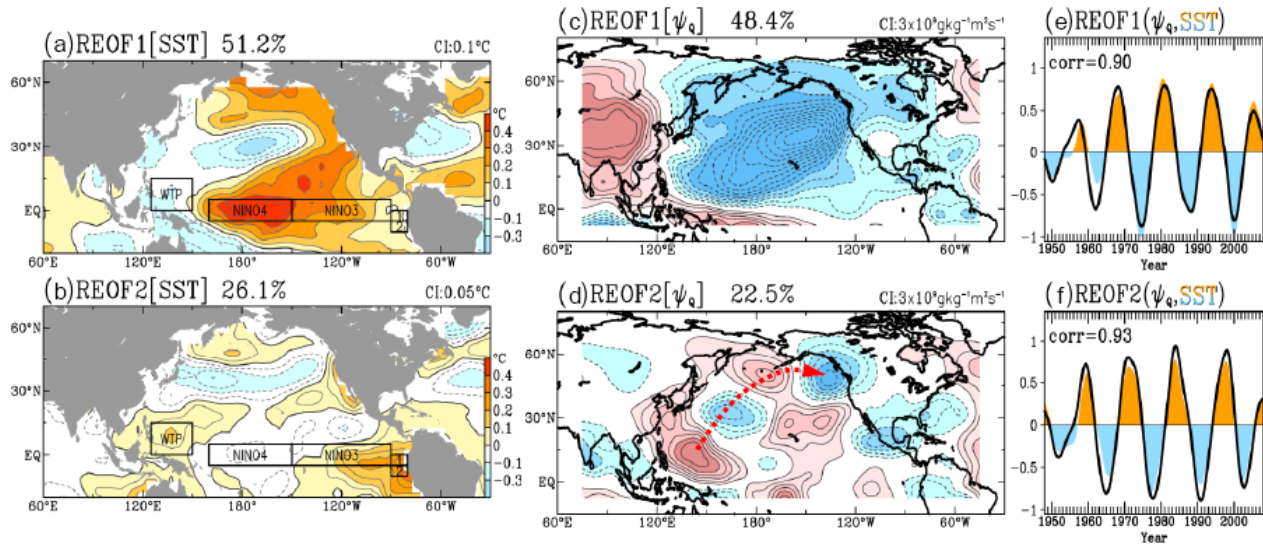


Fig. 5. (a) REOF 1 and (b) REOF 2 of the monthly Kaplan SST bandpassed by 10-15 year from 1948 to 2007. Contour interval is 0.1°C in (a) and 0.05°C in (b). (c) REOF 1 and (d) REOF 2 of the bandpassed column-integrated moisture flux streamfunction (ψ_Q). The normalized coefficients are shown in (e) and (f) as solid curves, with the coefficients of the bandpassed SST superimposed by shading; their correlation coefficients are shown in the upper left of (e) and (f). The teleconnection wave train is indicated by a red dashed arrow in panel (d).

4. Concluding remarks

Recurrent atmospheric circulation patterns develop over the Gulf of Alaska as a result of the teleconnection associated with the warm-to-cool and cool-to-warm transition phases of the Pacific QDO. These circulation patterns modulate transient synoptic activities over the western United States which, in turn,

lead to a 3 year lag in both the precipitation and the hydrological cycle of the GSL watershed. The GSL elevation responds to such precipitation variations with a 3 year lag and therefore, it takes on average 6 years for the GSL elevation to respond to the warm/cool phases of the Pacific QDO. Such atmospheric and hydrological processes create a half-phase delay of the GSL elevation from the Pacific QDO, leading to their out-of-phase relationship as was shown in Fig. 1.

A proper monitoring of the status of the Pacific QDO evolution can therefore serve in part to predict the precipitation tendencies in the Great Basin and so, foretell the GSL elevation for future years. A conceptual model for such an application of the science was illustrated in Fig. 3.

References

- Allan, R., 2000: ENSO and climatic variability in the last 150 years, *El Niño and the Southern Oscillation: Multiscale Variability, Global and Regional Impacts*, H. F. Diaz and V. Markgrav Ed., Cambridge Univ. Press, Cambridge, U.K, pp. 3–56.
- Allan, R. J., and T. J. Ansell, 2006: A new globally-complete monthly historical gridded mean sea level pressure data set (HadSLP2): 1850-2004, *J. Climate*, **19**, 5816-5842.
- Chen, T.-C., 1985: Global water vapor flux and maintenance during FGGE. *Mon. Wea. Rev.*, **113**, 1801–1819.
- Dettinger, M. D., D. R. Cayan, H. F. Diaz, and D. M. Meko, 1998: North–south precipitation patterns in western North America on interannual-to-decadal timescales. *J. Climate*, **11**, 3095–3111.
- Gershunov, A., and T. P. Barnett, 1998: Interdecadal modulation of ENSO teleconnections. *Bull. Amer. Meteor. Soc.*, **79**, 2715–2725.
- Iacobucci, A. and A. Noullez, 2005: A frequency selective filter for short-length time series, *Computational Economics*, **25**, 75-102.
- Kalnay, E., and Co-Authors, 1996: The NCEP/NCAR 40-year reanalysis project, *Bull. Amer. Meteor. Soc.*, **77**, 437-470.
- Kaplan, A., M. Cane, Y. Kushnir, A. Clement, M. Blumenthal, and B. Rajagopalan, 1998: Analyses of global sea surface temperature 1856-1991, *J. Geophys. Res.*, **103**, 567-589.
- Lall, U., and M. Mann, 1995: The Great Salt Lake: A barometer of low-frequency climatic variability, *Water Resour. Res.*, **31**, 2503-2515.
- Legates, D. R. and C. J. Willmott, 1990: Mean seasonal and spatial variability in gauge-corrected, global precipitation. *Int. J. Climatol.*, **10**, 111-127.
- Mann, M. E., Park, J., 1996: Greenhouse warming and changes in the seasonal cycle of temperature: Model versus observation, *Geophys. Res. Lett.*, **23**, 1111-1114.
- Tourre, Y. M., B. Rajagopalan, Y. Kushnir, M. Barlow, and W. B. White, 2001: Patterns of coherent decadal and interdecadal climate signals in the Pacific Basin during the 20th Century. *Geophys. Res. Lett.*, **28**, 2069.
- Wang, S.-Y., R. R. Gillies, J. Jin, and L. E. Hips, 2009a: Coherence between the Great Salt Lake level and the Pacific quasi-decadal oscillation, *J. Climate* (in press), DOI: 10.1175/2009JCLI2979.1
- _____, _____, L. E. Hips, and J. Jin, 2009b: A transition-phase teleconnection of the Pacific QDO, *Climate Dynamics* (<http://cliserv.jql.usu.edu/paper/CD/pacific-qdo.pdf>).
- White W. B., and Z. Liu, 2008a: Non-linear alignment of El Niño to the 11-yr solar cycle, *Geophys. Res. Lett.*, **35**, L19607, doi:10.1029/2008GL034831.
- _____, and _____, 2008b: Resonant excitation of the quasi-decadal oscillation by the 11-year signal in the Sun’s irradiance, *J. Geophys. Res.*, **113**, C01002.
- Zhang, Y., J. M. Wallace, and D. S. Battisti, 1997: ENSO-like interdecadal variability: 1900–93. *J. Climate*, **10**, 1004–1020.